Single-Spin Echo Multiband Diffusion Imaging with Slice Select Gradient Reversal

Matthew J. Middione[1], Hua Wu[2], Robert F. Dougherty[2], Kangrong Zhu[3], Adam B. Kerr[3], and John M. Pauly[3]
[1]*Applied Sciences Laboratory West, GE Healthcare, Meno Park, CA, United States,* [2]*CNI, Stanford University, Stanford, CA, United States,* [3]*Electrical Engineering, Stanford University, Stanford, CA, United States*

PURPOSE: Echo planar imaging (EPI), especially single shot EPI, is the method of choice for diffusion MRI (dMRI) due to its short scan time and motion insensitivity. However, it is sensitive to chemical-shift artifacts due to the low bandwidth in the phase-encoding direction[1], which requires the use of efficient fat suppression to remove fat ghosting in the phase encode direction. These fat ghosts can lead to quantitative inaccuracies in dMRI metrics. Single-spin-echo (SSE) sequences combined with standard fat saturation techniques can be inefficient in eliminating chemical shift artifacts while system limitations generally impose less than desired spatial selectivity for a spectral spatial water-only excitation based approach. Dual-spin-echo (DSE) sequences, which use two refocusing pulses and bipolar diffusion gradients[2] can be combined with fat saturation and a slice-selection gradient reversal (SSGR) method[3], which uses slice-selection gradients of opposing polarity for the two refocusing pulses, for efficient fat suppression and high spatial selectivity. DSE, however, results in an increased TE and TR, which reduces the signal-to-noise ratio (SNR) and can prolong scan duration compared to conventional SSE sequences. The purpose of this study was to implement a SSE dMRI sequence using Multiband (MB) imaging and SSGR to provide efficient fat suppression with increased SNR compared to DSE without having to compromise on the minimum slice thickness.

METHODS: All scanning was conducted using a 3.0T Discovery MR750 scanner (GE Healthcare, Waukesha, WI) using a 32-channel head coil (Nova Medical, Wilmington, MA). All images were acquired using a spin-echo EPI diffusion weighted sequence with the following imaging parameters: 25.6cm^2 FOV, 128x128 matrix, 2.0x2.0x3.0mm^3 resolution, 90mm of coverage in the slice dimension, 10 T2 (b_0) images, 30 diffusion encodings with b_{max} = 1000 s/mm^2, and 2x in-plane parallel imaging. Data were acquired using 1) SSE without any form of fat saturation or suppression; 2) SSE with a spatially non-selective fat saturation pulse (FatSat); 3) SSE with a spectral spatial (SpSp) fat suppression pulse; 4) DSE with FatSat and SSGR; and 5) The proposed SSE MB sequence with FatSat and SSGR and NEX=2. The slice thickness was kept constant for all sequences and chosen to be the minimum achievable for the SSE SpSp scan. The minimum achievable slice thickness for all non-SpSp scans was otherwise 0.8mm. The TE and TR were also minimized for each sequence. SSGR was implemented in the proposed MB sequence by inverting the slice select gradient polarity for the excitation pulse, thereby ensuring that the fat signal is not fully refocused. For the proposed MB sequence, a through-plane slice acceleration factor of 3 and blipped-CAIPI[4] with FOV/3 shift between adjacent slices was employed. The MB data were reconstructed using an in-house reconstruction framework in Matlab (The MathWorks Inc., Natick, MA), which utilized a 1D-GRAPPA reconstruction algorithm[5]. All non-DSE scans used the vendor provided prospective high order eddy current mitigation strategy[6] to reduce direction dependent image distortions due to eddy currents generated by the diffusion gradients. Temporal SNR maps were calculated from the 10 T2 images by dividing the mean signal within the T2 images in the temporal dimension by the standard deviation of the signal within the T2 images in the temporal dimension.

RESULTS: The results of this study are shown in Figure 1. Qualitatively, the image quality of the diffusion images look comparable across all scans (apart from the fat ghosting). Significant fat ghosting can be see for the SSE sequence while residual fat ghosting is still seen for the SSE FatSat sequence. SSE SpSp, DSE FatSat SSGR, and SSE MB FatSat SSGR all show no residual fat ghosting. The SNR maps show that the proposed SSE MB FatSat SSGR sequence with NEX = 2 provides comparable SNR to the SSE scan, despite the 3x reduction in TR. Although not presented, the use of SSGR in the SSE MB sequence alone causes roughly a 5% drop in overall SNR. While this is certainly undesirable, the slight reduction in SNR is acceptable given the benefit of reduced fat ghosting. The increased background noise in the MB SNR maps is likely due to choice of reconstruction[7].

DISCUSSION AND CONCLUSION: Sufficient fat suppression is needed for accurate DTI measurements. Fat saturation alone in SSE sequences is insufficient while SSE with a spectral spatial pulse results in proper fat suppression with limitations on the minimum slice thickness[8]. DSE with fat saturation and SSGR can achieve proper fat suppression at the expense of TE/TR and SNR. MB combined with fat saturation and SSGR can provide efficient fat suppression with increased SNR compared to DSE and comparable SNR compared to SSE without having to compromise on the minimum slice thickness.

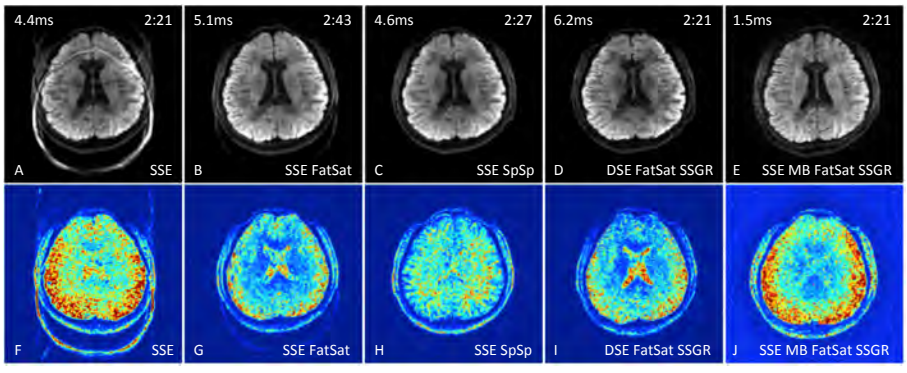

Figure 1. Representative diffusion images for b=1000 s/mm^2 (A-E) and temporal SNR maps (F-J) for SSE without any form of fat saturation or suppression (A,F), SSE with a non-selective fat (FatSat) saturation pulse (B,G), SSE with a spectral spatial (SpSp) fat suppression pulse (C,H), DSE with FatSat and slice-selection gradient reversal (SSGR) (D,I), and the proposed SSE MB sequence with FatSat, SSGR, and NEX=2 (E,J). The scan times and TR for each sequence are displayed in the upper-right and left corner, respectively, of the diffusion images. The SNR maps are scaled from [0 100].

REFERENCES: **1**. Fischer et al., Berlin: Springer-Verlag; 1998. 179-200. **2**. Reese et al., MRM 2003; 49:177-182. **3**. Nagy et al., MRM 2008; 60:1256-1260. **4.** Setsompop K. et al. MRM 2012; 67:1210-1224. **5**. Blaimer et al., JMRI 2006; 24:444-450. **6**. Xu et al., MRM 2013; 70(5):1293-305. **7.** Sotiropoulos el al., MRM 2013; 70(6):1682-1689. **8.** Sotiropoulos el al., Neuroimage 2013; 80:125-43.